Process Biochemistry xxx (xxxx) xxx–xxx

Contents lists available at ScienceDirect

Process Biochemistry

journal homepage: www.elsevier.com/locate/procbio

# A Novel esterase from *Pseudochrobactrum asaccharolyticum* WZZ003: Enzymatic properties toward model substrate and catalytic performance in chiral fungicide intermediate synthesis

Feng Cheng[a,1], Feifei Cheng[a,1], Jianyong Zheng[a], Guanzhong Wu[b], Yinjun Zhang[a,*], Zhao Wang[a]

[a] Key Laboratory of Bioorganic Synthesis of Zhejiang Province, College of Biotechnology and Bioengineering, Zhejiang University of Technology, Hangzhou, 310014, China
[b] Yifan Biotechnology Group Co. Ltd., Wenzhou, 32500, China

ARTICLE INFO

*Keywords:*
Esterase
(*R*,*S*)-DMPM
Metalaxyl
High activity
High enantioselectivity

ABSTRACT

Only a few esterases have been used for the synthesis of optically pure fungicide. For example, (*R*)-metalaxyl synthesized using esterase-involved bioreaction displays fungicide activity, whereas (*S*)-enantiomer is redundant. However, the biosynthesis of (*R*)-metalaxyl is currently hampered by the lower activity, selectivity and thermostability of esterase. Therefore, to obtain a better biocatalyst, several esterase genes were cloned from *Pseudochrobactrum asaccharolyticum* WZZ003. The esterase PAE07, among eight enzymes, was selected because it exhibited the highest hydrolysis activity toward (*R*,*S*)-DMPM. The DNA and amino acid sequence analysis suggested that PAE07 is a new member of lipolytic enzyme family V. The enzymatic properties of PAE07 toward (*R*,*S*)-DMPM and model substrate (*p*-nitrophenyl acetate) were investigated. PAE07 was found to be a highly active esterase with excellent enantioselectivity. The reaction conditions including temperatureand pH were optimized, and the effects of metal ions, organic solvents and detergents were also investigated. Results indicated that PAE07 is a competitive candidate for (*R*)-metalaxyl manufacturing.

## 1. Introduction

Esterases (EC 3.1.1.X), which catalyze esterification, ester hydrolysis, transesterification and acylation, are one of the most widely applied enzymes in white biotechnology [1–4]. These esterase-catalyzed reactions have many attractive properties, such as high chemo-, regio-, and stereo- selectivity, and do not require cofactors. Thus, esterases as potential biocatalysts have been used to produce enantiopure compounds in food, pharmaceutical and agrochemical industries [5–7].

Optically pure fungicides exhibit higher safety than the racemic ones (different enantiomers usually demonstrate distinct biological activities). For instance, (*R*)-enantiomer exhibits fungicide activity, while (*S*)-enantiomer is redundant or even harmful [8,9]. Mefenoxam, an efficient chiral-fungicide produced by Novartis has been widely used in seed treatment, foliar spray and broadcast soil applications. This fungicide is the (*R*)-enantiomer of metalaxyl fungicide (full name: methyl *N*-(2,6-dimethylphenyl)-*N*-(methoxyacethyl)-D-alaninate). Methyl(*R*)-N-(2,6-dimethylphenyl)-alaninate ((*R*)-DMPM) is the key intermediate to (*R*)-metalaxyl; therefore, o(*R*)-DMPM synthesis is the research hotspot for chiral fungicide synthesis [10].

Traditionally, the chemical synthesis of (*R*)-DMPM and its derivatives requires toxic or chiral catalysts [11], which are not environmentally friendly and not suitable for scale-up. The enzymatic kinetic resolution process of (*R*,*S*)-DMPM is high stereoselective and environmentally friendly but still at the laboratory research stage. A study isolated and characterized stereoselective lipases from *Burkholderia* sp. and identified five lipases possessing different enantioselectivities for racemic DMPM hydrolysis [12]. Among them, lipase MC 16-3 yielded 91.8% enantiomeric excess of the product ($e.e._p$) of (*R*)-DMPM at 25% conversion and lipase 99-2-1 yielded 91.0% $e.e._p$ of (*R*)-DMPM at 30% conversion. In another study, immobilization of lipase PS was employed and yielded a high conversion (> 80%) and a satisfactory enantiomeric excess (96% $e.e._p$) [13]. However, for the large scale-up of this bioprocess, the currently used lipase exhibits several shortcomings such as insufficient activity, selectivity, thermostability, and organic solvent tolerance. Therefore, a novel, highly active, highly enantioselective, and robust esterase is greatly desired.

In a previous study, a *Pseudochrobactrum asaccharolyticum* WZZ003 was isolated from soil sample and identified as a candidate for (*R*)-DMPM synthesis (see the route for (*R*)-DMPM synthesis in Fig. 1). In the current study, the gene of esterase PAE07 was mined and cloned from *P. asaccharolyticum* WZZ003, and successfully heterogeneously expressed

* Corresponding author at: College of Biotechnology and Bioengineering, Zhejiang University of Technology, Chaowang Road 18, Hangzhou, 310014, China.
*E-mail address:* zhangyj@zjut.edu.cn (Y. Zhang).
[1] These authors contributed equally to this work.

https://doi.org/10.1016/j.procbio.2018.03.011
Received 25 December 2017; Received in revised form 6 March 2018; Accepted 15 March 2018

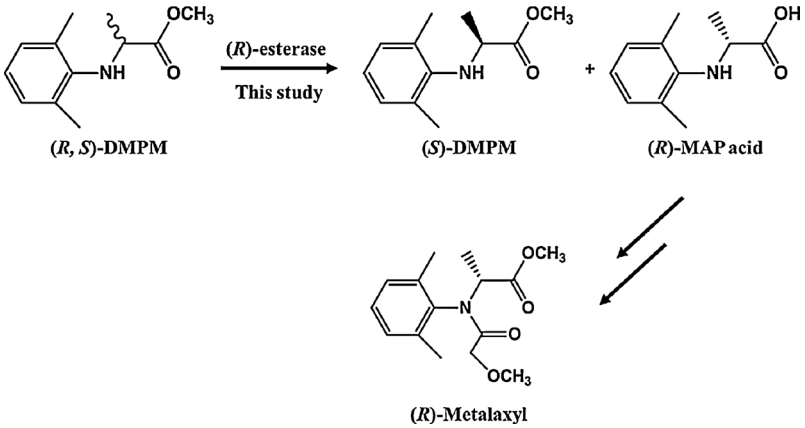


**Fig. 1.** Enzymatic resolution of (*R*,*S*)-DMPM.

in *Escherichia coli* BL21(DE3). This gene encoding enzyme (PAE07) exhibited high hydrolysis activity toward (*R*,*S*)-DMPM with excellent enantioselectivity. The enzymatic properties of PAE07 including optimal temperature and pH of its enzymatic reaction, and the effects of metal ions, organic solvents and detergents were investigated. The kinetic parameters ($k_{cat}$ value and $K_M$ value) and specific activity of PAE07 toward (*R*,*S*)-DMPM and model substrate *p*-nitrophenyl acetate (*p*-NPA) were detected and compared with those of other excited lipases.

## 2. Materials and methods

### 2.1. Chemicals, enzyme and kits

All chemicals were of analytical-reagent grade or higher quality and were purchased from Sigma-Aldrich or Aladdin Co., Ltd. (Shanghai, China) unless stated otherwise. Racemic methyl-(*R*,*S*)-N-(2,6-dimethylphenyl)-alaninate and (*R*,*S*)-N-(2,6-dimethylphenyl)alanine was purchased from Zhejiang Heben Chemical Co., Ltd (Zhejiang, China). DEAE Sepharose™ Fast Flow and Phenyl Sepharose™ 6 Fast Flow were purchased from GE Healthcare Co., Ltd. (Shanghai,China). TransStart™ Taq DNA Polymerase was purchased from TransGen Biotech Co., Ltd. (Beijing, China).

### 2.2. Strains and plasmids

*Pseudochrobactrum asaccharolyticum* WZZ003 strain was isolated from soil sample and deposited in China Center for Type Culture Collection (CCTCC M2014209). pEASY-blunt vector (TransGen Biotech Co., Ltd, Beijing, China) was used for *pae* gene cloning and expression. *E. coli* DH5α and BL21(DE3) chemically competent cells purchased from TransGen Biotech Co., Ltd (Beijing, China) were applied to the plasmid transformation experiment as a cloning host and an expression host, respectively.

### 2.3. Gene cloning, heterogeneous expression, and purification of PAE07

Sequence alignment was performed using a multiple-alignment program (ClustalW) [14]. The primer was designed according to the *N*-terminal and *C*-terminal amino acid sequences of the predicated α/β hydrolases from *Pseudochrobactrum* sp. AO18b and *Pseudochrobactrum* sp. B5. PCR was conducted out as follows: denaturation of DNA template at 94 °C for 5 min; 30 cycles at 94 °C for 30 s, 54 °C for 30 s, and 72 °C for 1 min; and final extension at 72 °C for 10 min. The PCR products were purified using the Genomic DNA Fragment Rapid Purification Kit (BioDev-Tech, Beijing, China) and were inserted into a pEASY-blunt vector. The ligated product pEASY-blunt-*pae* was then transformed into *E. coli* DH5α competent cells. The plasmid pEASY-blunt-*pae* isolated from the harvested cells was transformed into competent *E. coli* BL21(DE3). The *E. coli* BL21(DE3) harboring pEASY-blunt-*pae* was grown in LB media supplemented with ampicillin at 37 °C at 200 rpm. When the $OD_{600}$ reached 0.6–0.8, isopropyl-β-D-thiogalactopyranoside (IPTG) was added to a final concentration of 0.2 mM to induce the gene expression at 22 °C for 8 h.

The harvested cells were resuspended in 50 mM of Tris-HCl (pH 8.0) and disrupted by sonication and the cell lysate was centrifuged for 5 min. The resulting crude enzyme solution was loaded onto a Ni-NTA column (1 ml, Bio Basic Inc), and the retained protein was gradually eluted with an increasing gradient of imidazole from 10 mM to 250 mM at a flow rate of 1 ml/min. The resulting enzyme fractions were analyzed using sodium dodecyl sulfate polyacrylamide gel electrophoresis (SDS-PAGE). A Thermo Scientific Pierce BCA protein assay kit (Shanghai, China) was used to quantify the proteins as previously reported [15]. The purified solution was stored at −20 °C for further characterization.

### 2.4. Enzyme assay

The recombinant enzyme activity was measured. A total of 1 mM *p*-NPA was hydrolyzed to *p*-nitrophenol (*p*-NP) at 40 °C in 50 mM of Tris-HCl (pH 8.0) and was assayed by spectrophotometry at 405 nm. One unit of enzyme activity (U) was defined as the amount of enzyme releasing 1.0 μmol of *p*-NP per minute [16].

### 2.5. Substrate specificity

The substrate specificity was evaluated using *p*-NP esters with different chain lengths ($C_2$–$C_{16}$) dissolved in isopropanol to a final concentration of 0.33 mM. The reaction mixtures consisted of purified PAE, 0.33 mM *p*-NP ester and 50 mM Tris-HCl (pH 8.0). The reactions were conducted at 35 °C for 5 min and terminated of the reactions was by adding acetonitrile [17,18]. The enzyme activity was determined by measuring the absorbance at 405 nm [19]. Denatured PAE07 was added to the reaction as a negative control.

### 2.6. Effect of pH and temperature on the activity and stability of PAE07

To investigate the effects of pH and temperature on the enzyme activity, the initial hydrolysis rate of *p*-NPA was measured under various reaction conditions. The optimum pH was determined in the following buffers: 50 mM sodium citrate buffer (pH 3.0–5.0), 50 mM sodium phosphate buffer (pH 6.0–8.0), 50 mM Tris-HCl buffer (pH 9.0), and $Na_2CO_3$-$NaHCO_3$ (pH 10.0–11.0). The reaction mixture was agitated for 2 h at 40 °C. The optimal temperature of the enzymatic reaction was investigated by measuring the residual activities at 20–70 °C for 30 min. The stability of PAE07 was measured at different

temperature (30, 40, 50, 60 and 70 °C) for 2 h. The residual activities were measured every 30 min using the standard enzyme assay.

### 2.7. Kinetic study of PAE07 for the determination of $K_M$, $V_{max}$, and $k_{cat}$ values

The reaction velocities of hydrolyzing *p*-NPA at different substrate concentrations (0.01–1 mM) were determined for 5 min at 40 °C and pH 8.0. The kinetic parameters of PAE07 was calculated by adding 1.66 mg/mL of pure enzyme to each assay. The relationship between initial velocity and substrate concentration was fitted to the Lineweaver-Burk plot, and the Michaelis-Menten constant ($K_M$), maximum velocity ($V_{max}$), and catalytic constant ($k_{cat}$) were also calculated.

### 2.8. Effect of metal ions, organic solvents, and surfactants on the enzyme activity of PAE07

A concentration of metal ions ($Na^+$, $K^+$, $Ca^{2+}$, $Fe^{2+}$, $Zn^{2+}$, $Mg^{2+}$, $Ba^{2+}$, $Cu^{2+}$, $Mn^{2+}$, $Co^{2+}$, $Ni^{2+}$, and $Al^{3+}$) and ethylenediaminetetraacetic acid (EDTA) were added to a final concentration of 1 and 5 mM. The reaction mixtures were incubated at 40 °C for 30 min, and the residual enzyme activity was measured at the end of the reaction. The solution without metal ions was regarded as a control.

The PAE07 was incubated in the presence of various organic solvents (glycerol, DMSO, DMF, methanol, acetonitrile, ethanol, acetone, isopropanol, tetrahydrofuran, *n*-butanol, chloroform, toluene, and *n*-hexane) at 10% and 30% (v/v) in a water bath at 40 °C for 30 min, and then the residual enzyme activity was measured.

A solution was incubated in the presence of detergents (namely, EDTA, SDS, Tween 20, Tween 80, Triton X-100, and Urea at 1% and 5% (v/v) for 30 min. The residual enzyme activities were assayed by the standard enzyme assay.

### 2.9. Enantioselectivity toward methyl(R,S)-N-(2, 6-dimethylphenyl)-alaninate

The purified PAE07 was used in catalyzing a target substrate and compared with commercial enzymes. Enzymatic reactions were performed in the mixture, which consisted of optical methyl(*R,S*)-N-(2,6-dimethylphenyl)-alaninate and an enzyme solution dissolved in 50 mM Tris-HCl (pH 8.0), at 40 °C. The hydrolytic activity and enantiomeric excesses (*e.e.*) were measured using HPLC with a chiral Ultimate® Cellud-Y column (0.5 ml/min, 4.6 × 250 mm, *n*-hexane/*iso*PrOH/Trifluoroacetic acid = 98:2:0.1) at 220 nm. The retention times for the enantiomers of DMPM were $t_S(S)$ = 10.406 min and $t_S(R)$ = 9.909 min, and the resulting retention times of product were $t_P(S)$ = 32.178 min and $t_P(R)$ = 24.283 min. One unit of enzyme activity was defined as the amount of enzyme that produces 1 μmol/min of MAP acid.

### 2.10. Effect of substrate concentration on the hydrolysis of (R,S)-DMPM

The reactions, including 1.65 mg $ml^{-1}$ of purified PAE07, 50 mM sodium phosphate (pH = 8.0), and a series of concentration gradients (19–200 mM), were conducted at 40 °C for 10 min. Initial reaction rate was determined by the conversion of substrate. At a low substrate concentration, the kinetic constants of PAE were calculated from the Lineweaver-Burk plot.

### 2.11. Homology modelling and docking

A maximum-likelihood tree was constructed using Molecular Evolutionary Genetics Analysis software (MEGA 7) by analyzing the relationship between PAE07 and other lipolytic enzymes [20,21]. The homology model of PAE07 was generated using the HHpred Server and MODELLER [22]. The crystal structures of *N*-acyl homoserine lactonase with *N*-butanoyl homoserine (chain A of 4G9E and 4G8D) were retrieved from the PDB database [23]. The sequence identity of PAE07 toward 4G9E, 4G8D, and other selected esterase was determined using ClustalW. Docking was performed using AutoDock Vina to predict the binding energy and fine tune the ligand placement in the binding site under the default docking parameters, in which point charges were initially assigned according to the AutoDock semi-empirical force field [24,25].

## 3. Results and discussion

### 3.1. Hunting for esterase gene from the genome of P. asaccharolyticum WZZ003

In our previous work, the WZZ003 strain that can enantioselectively hydrolyze (*R,S*)-DMPM to (*R*)-MAP-acid was isolated from 425 soil samples, and identified as *P. asaccharolyticum* based on a 16S rDNA phylogenetic tree analysis and physiological-biochemical characterizations. Although the genome sequence of *P. asaccharolyticum* was not available in the NCBI database, two genomic sequences of closely related species (*Pseudochrobactrum* sp. B5 and *Pseudochrobactrum* sp. AO18b) were used as references for the analysis. The functional prediction identified 16 (in the genomic B5) and 13 (in the genomic AO18b) candidate genes encoding lipases/esterases, respectively. Twenty-nine pairs of primers were designed for the amplification of the lipase/esterase genes from the genome DNA of *P. asaccharolyticum* WZZ03. Eight genes were successfully cloned from *P. asaccharolyticum* WZZ003 and expressed in *E. coli* BL21(DE3) (data not shown). Among them, the enzyme PAE07 displayed the highest conversion and excellent enantioselectivity (*e.e.* > 99%) toward (*R,S*)-DMPM (Fig. 1 and Table S1). Consequently, this enzyme was selected as a potential biocatalyst for further studies.

### 3.2. DNA and amino acid sequence analysis of PAE07

The gene of PAE07 contained an of 813 bp ORF encoding a 270-amino acid protein. The nucleotide sequence of PAE07 has been deposited in the GenBank database (accession no. MF591571). The online tools BlastN and BlastP were used to obtain similar sequences of this protein. The BlastN analysis could not find any sequences with significant similarity to the *pae*07 gene. The BlastP results showed that only two amino acid sequences of proteins shared high homology (> 50%) with PAE07, i.e., alpha/beta hydrolase from *Pseudochrobactrum* sp. AO18b (WP_022712336.1) and alpha/beta hydrolase from *Pseudochrobactrum* sp. B5 (WP_075655351.1) at 92% and 91% sequence identities, respectively. The phylogenetic analysis of esterase PAE07 was conducted based on the amino acid sequences of different lipolytic enzymes belonging to families I–VIII obtained from the GenBank database. As shown in Fig. 2, esterase PAE07 is in close proximity to the lipolytic enzymes which belong to family V (lipolytic enzymes from *Streptomyces* sp. and *Sulfolobus acidocaldarius*). The multiple sequence alignment (Fig. S1) revealed the conserved catalytic triad of Asp220, His249 and Ser99 and the GxHxG motif. These results indicated that esterase PAE07 is a new member of lipolytic enzyme family V.

### 3.3. Expression and purification of PAE07

The *E. coli* BL21 (DE3) cells harboring pEASY-blunt-*pae*07 were used to express active PAE07. The esterase activity determination indicated that the recombined PAE07 was successfully expressed in *E. coli* and the expression level of PAE07 was estimated using SDS-PAGE analysis (Fig. S2a). On the basis of C-terminal 6 × His affinity tag, esterase PAE07 was purified using the Ni-NTA Sepharose column. After purification, esterase PAE07 was loaded on SDS-PAGE and was separated as a single protein consistent with the predicted molecular weight (29.7 kDa) (Fig. S2b).

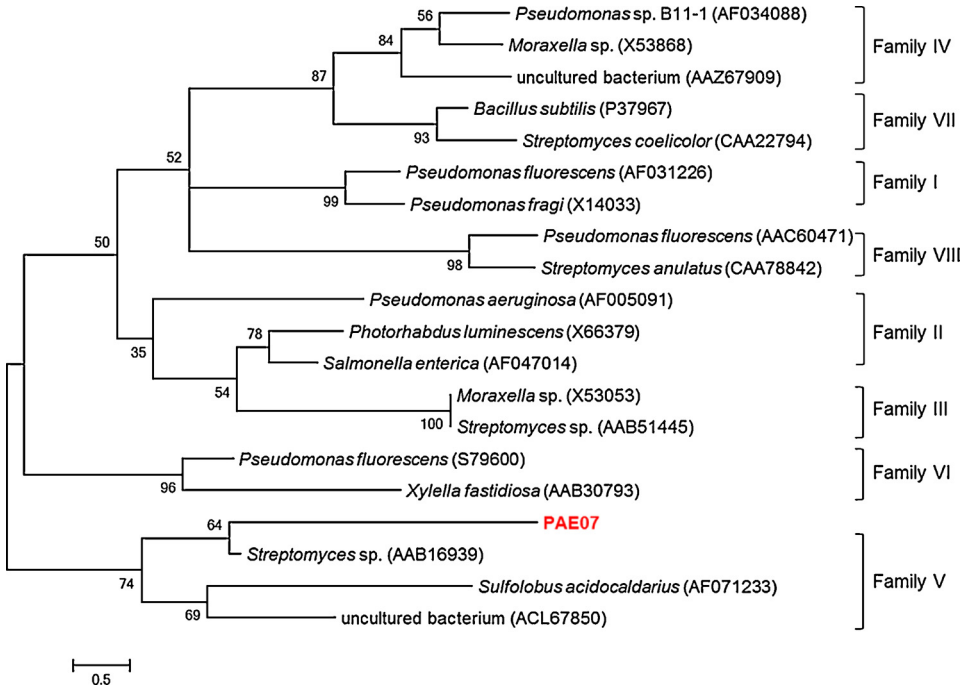


**Fig. 2.** Maximum-likelihood phylogenetic tree. The phylogenetic analysis was conducted using the MEGA 7 software, and the esterase PAE07 is shown in red color. (For interpretation of the references to colour in this figure legend, the reader is referred to the web version of this article.)

### 3.4. Substrate specificity of PAE07 toward p-NP esters

The substrate specificity of PAE07 was investigated using a broad range of *p*-NP esters with different acyl chain lengths (C2–C16) as substrates. PAE07 displayed the highest activity toward *p*-nitrophenyl caproate (C6, 100%, set as reference) and *p*-nitrophenyl caprylate (C8, 83%) (Fig. S3). PAE07 exhibited 64% and 65% relative activity on C2 and C4 esters, respectively, compared with *p*-nitrophenyl caproate (C6 substrate) (Fig. S3). However, the hydrolytic activity of PAE07 decreased dramatically with the elongation of carbon chains. The relative activity of PAE07 toward the C10 to C16 substrates were only < 30% compared with the C6 substrate. These results indicated that PAE07 is a "true" esterase that preferentially catalyzes the hydrolysis of short acyl chains.

### 3.5. Effect of pH and temperature on the activity and stability of PAE07 toward the model substrate

*p*-NPA is commonly used as a model substrate for characterization of lipases/esterases [16,26]. The influences of pH and temperature on PAE07 activity were investigated on *p*-NPA. Given that pH may affect the protein's conformation, the investigation of the effect of pH on the stability of enzyme is indispensable [27]. The changes in PAE07 activity along with a broad pH range (3.0–11.0) were shown in Fig. 3a. The enzyme exhibited the highest activity at pH 7.0–9.0, and maximal activity at pH 8.0. PAE07 demonstrated good pH- stability at pH 5.0–9.0. The residual activity of PAE07 remained more than 80% after 2 h incubation in this pH range (Fig. 3b).

The effects of different temperatures on the activity and stability of PAE07 were also investigated. The optimal temperature of PAE07 toward *p*-NPA was 40 °C, and the enzyme showed comparative activity between 30 and 50 °C. However, the enzyme activity significantly decreased when temperature increased above 50 °C (Fig. 3c). The stability of PAE07 was measured after incubation at 30, 40, 50, 60, and 70 °C for at different periods. The residual activity remained approximately 90% after 2 h of incubation at 30, 40 and 50 °C. When the incubation temperature increased to 60 °C, the activity remained above 60% after 2 h (Fig. 3d). Thus, PAE07 has good thermostability.

### 3.6. Effect of metal ions, organic solvents, and detergents on PAE07 activity

Metal ions are key factors that influence enzyme activity by interacting with the disulfide bond of enzyme structure, or binding to the substrate to form a salt [28–30]. The effects of metal ions on PAE07 were determined at 1 and 5 mM concentrations of a series of metal ions. The activity of PAE07 was affected by many of the metal ions and was strongly inhibited by $Cu^{2+}$, $Co^{2+}$, $Zn^{2+}$, $Fe^{2+}$, $Al^{3+}$, $Ag^{+}$ and $Hg^{2+}$ (Table 1). Given that $Ag^{+}$ and $Hg^{2+}$ strongly bind to sulfhydryl reagents, the thiol group was essential for PAE07's catalytic activity. $Na^{2+}$ and $Ca^{2+}$ slightly increased the activity of PAE07. Nevertheless, no inhibition was observed in the presence of chelating agent EDTA suggesting that PAE07 have no metal ion requirements for catalysis.

Esterase an industrial biocatalyst, commonly used in non-aqueous media such as organic solvents [31,32]. Thus, the effects of various organic solvents with different log *P* values on the enzyme activity were investigated at two different concentrations (10% and 30%, Table 2). Most of organic solvents exhibited a certain inhibition at low concentration (10%), but some exhibited a positive promotion. For instance, glycerol, DMSO and *n*-hexane weakly enhanced the enzyme activity at high concentration (30%). The other organic solvents showed evident negative influence.

The enzyme activity of PAE07 was detected with different concentrations of various detergents. As shown in Table 3, all surfactants exerted a certain inhibition on its activity. Urea, Triton X-100, Tween 20, and Tween 80 showed the inconspicuous effects on PAE07 activity at low level (1%) but exerted significant inhibition after concentration

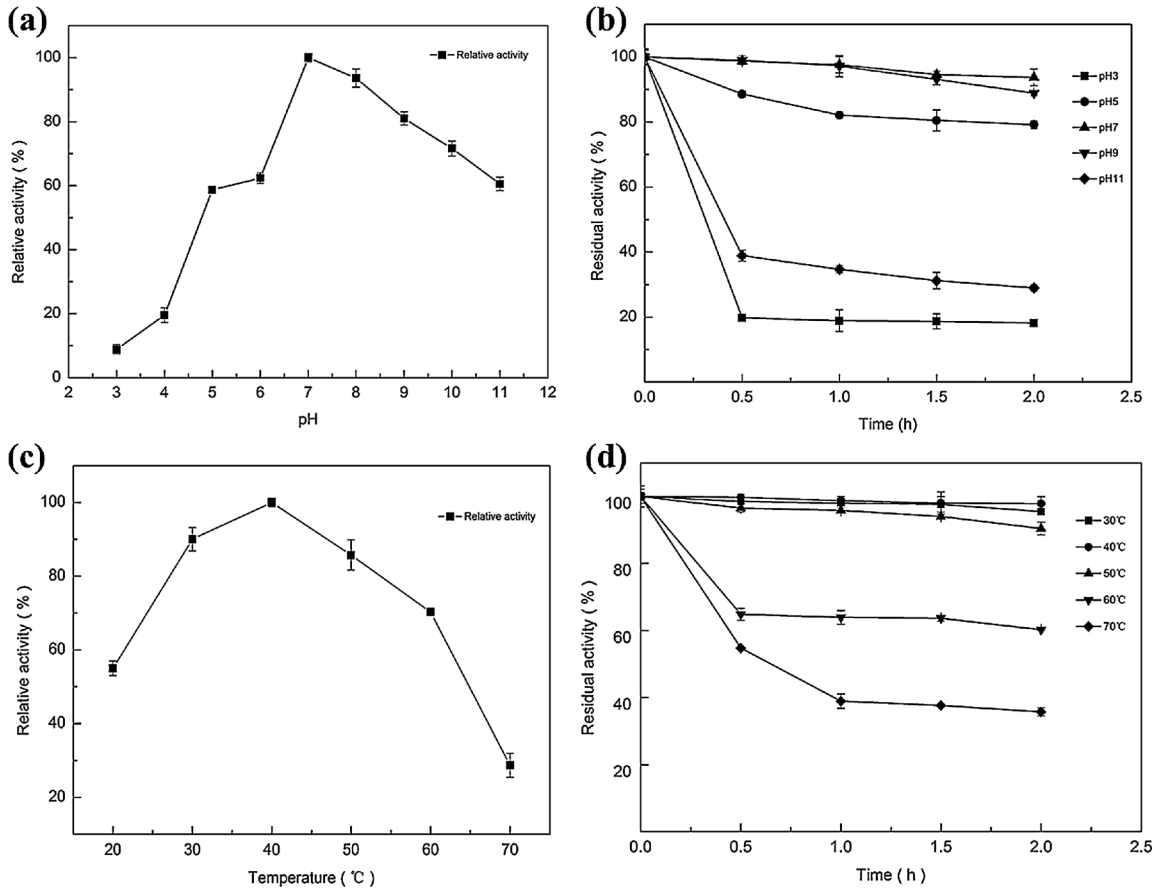


**Fig. 3.** Effect of pH and temperature on the activity and stability of PAE07. (a) Optimal pH for hydrolyzing *p*-NPA (sodium citrate buffer (pH 3.0–5.0), sodium phosphate buffer (pH 6.0–8.0), Tris-HCl buffer (pH 9.0), $Na_2CO_3$-$NaHCO_3$ (pH 10.0–11.0); (b) Enzyme stability at different pH (■ pH 3; ● pH 5; ▲ pH 7; ▼ pH 9; ♦ pH 11). (c) Optimal temperature for hydrolyzing *p*-NPA. (d) Thermostability was determined at different temperatures (■ 30 °C; ● 40 °C; ▲ 50 °C; ▼ 60 °C; ♦ 70 °C) from 0.5 to 2.0 h.

increase (5%). The residual activity remained only 48% after adding SDS. This finding revealed SDS exerted an apparent inhibition on PAE07 activity. DTT exhibited no effect on esterase PAE07 activity. This result suggested that the recombinant esterase has no disulfide bonds.

### 3.7. Specific activity and kinetic parameters of PAE07 toward p-NP esters

The specific activity of purified PAE07 to *p*-NPA (the model structure) was 421.0 U/mg protein, which was ~13-fold higher than the specific activities of esterases from *Aureobasidium pullulans* (31.8 U/mg)

**Table 1**
Effect of metal ions on PAE07 activity.

| Metal ion | % Relative activity (SD) | |
|---|---|---|
| | 1 mM | 5 mM |
| Control | 100.0 | 100.0 |
| $Na^+$ | 91.2 ± 5.3 | 105.8 ± 5.5 |
| $K^+$ | 93.8 ± 8.8 | 85.5 ± 5.2 |
| $Ca^{2+}$ | 98.2 ± 5.1 | 102.8 ± 6.7 |
| $Mg^{2+}$ | 97.6 ± 9.0 | 96.6 ± 1.4 |
| $Cu^{2+}$ | 18.3 ± 4.9 | 12.8 ± 3.3 |
| $Fe^{2+}$ | 75.9 ± 1.4 | 23.2 ± 0.3 |
| $Zn^{2+}$ | 13.3 ± 1.3 | 2.9 ± 0.1 |
| $Co^{2+}$ | 80.0 ± 5.6 | 46.2 ± 0.8 |
| $Mn^{2+}$ | 95.3 ± 1.6 | 94.7 ± 4.7 |
| $Ba^{2+}$ | 93.1 ± 1.8 | 83.7 ± 6.0 |
| $Ag^+$ | 29.8 ± 1.0 | 7.7 ± 0.7 |
| $Al^{3+}$ | 71.1 ± 1.5 | 24.9 ± 4.1 |
| EDTA | 101.9 ± 0.7 | 98.9 ± 1.2 |

The activity was calculated using the *p*-NPA assay at 40 °C and pH 8.0. The activity of PAE07 in the non-metal ion solution was the reference.

**Table 2**
Effect of organic solvents on PAE07 activity.

| Organic solvents | Log $P_{ow}$ | % Relative activity ( ± SD) | |
|---|---|---|---|
| | | 10% (v/v) | 30% (v/v) |
| Control | – | 100.0 | 100.0 |
| Glycerol | −1.76 | 111.9 ± 3.4 | 103.8 ± 5.6 |
| DMSO | −1.35 | 106.6 ± 4.8 | 110.6 ± 4.4 |
| DMF | −1.0 | 49.0 ± 6.3 | 31.2 ± 0.3 |
| Methanol | −0.76 | 42.6 ± 2.6 | 18.3 ± 1.9 |
| Acetonitrile | −0.34 | 39.0 ± 1.5 | 8.4 ± 0.5 |
| Ethanol | −0.3 | 133.3 ± 1.6 | 45.2 ± 1.2 |
| Acetone | −0.24 | 99.1 ± 4.9 | 33.7 ± 0.7 |
| Isopropanol | 0.38 | 69.3 ± 1.5 | 15.6 ± 0.4 |
| Tetrahydrofuran | 0.49 | 9.9 ± 0.9 | 2.4 ± 2.9 |
| *n*-butanol | 0.88 | 79.3 ± 9.7 | 76.9 ± 7.9 |
| Chloroform | 1.97 | 75.7 ± 10.7 | 19.9 ± 11.7 |
| Toluene | 2.73 | 36.4 ± 2.3 | 32.2 ± 2.8 |
| *n*-hexane | 3.5 | 117.1 ± 8.6 | 105.9 ± 12.5 |

The activity was determined using *p*-NPA at 40 °C and pH 8.0. The activity of PAE07 in non-organic solvents was defined as 100%.

**Table 3**
Effect of detergents on PAE07 activity.

| Detergents | % Relative activity (SD) | |
|---|---|---|
| | 1% (v/v) | 5% (v/v) |
| None | 100 | 100 |
| Urea | 87 ± 7.3 | 65 ± 4.3 |
| SDS | 48 ± 4.5 | 37 ± 5.7 |
| Trtion-X100 | 88 ± 6.9 | 57 ± 5.7 |
| Tween20 | 94 ± 4.5 | 82 ± 3.4 |
| Tween80 | 95 ± 6.6 | 87 ± 4.5 |
| DTT | 99 ± 3.6 | 97 ± 6.9 |

The activity was determined using *p*-NPA at 40 °C and pH 8.0. The activity of PAE07 in non- detergents solvents was defined as 100%.

[33] and *Bacillus pumilus* PS213 (32 U/mg) [34]. The $K_M$ and $k_{cat}$ values of PAE07 toward *p*-NPA were determined as 0.66 ± 0.03 mM and 70.2 ± 4.3 $s^{-1}$, respectively.

### 3.8. The specific activity and kinetic parameters of PAE07 and commercialized enzymes toward (R,S)-DMPM

To date, only five esterases, including PAE07, have been identified to enantioselectively hydrolyze racemic DMPM [10,13]. The specific activity and enantioselectivity of PAE07 and other four commercialized enzymes were evaluated on 38 mM racemic DMPM. Three out of the five enzymes, i.e., PAE07, lipase PS, and Amano lipase AK, showed excellent $e.e._p$ values (99.9%), and others displayed low $e.e._p$ values (89.6% for Alcalase and 26.0% for Novozym 435, Table S2). PAE07 exhibited the highest specific activity (764 U/mg), which was 54.6-fold and 127.3-fold higher than that of lipase PS (14 U/mg) and Amano lipase AK (6 U/mg), respectively (Table S2). The kinetic parameters of PAE07 and commercialized lipase PS were also tested. The $k_{cat}$ and $K_M$ values of PAE07 to (*R,S*)-DMPM were $1.08 \times 10^7$ $s^{-1}$ and 34.3 mM, respectively, and the $k_{cat}$ and $K_M$ values of lipase PS were $1.15 \times 10^7$ $s^{-1}$ and 87.5 mM, respectively. The catalytic efficiency $k_{cat}/K_M$ value of PAE07 was 315 $\mu M^{-1}s^{-1}$, which was ~2.4-fold higher than that of lipase PS (130 $\mu M^{-1}s^{-1}$). To the best of our knowledge, PAE07 had the highest activity and catalytic efficiency toward (*R,S*)-DMPM among all enzymes. This result suggested that PAE07 is a competitive biocatalyst candidate for the large-scale production of (*R*)-DMPM and (*R*)-metalaxyl in a large scale.

### 3.9. Time course of enzymatic hydrolysis reaction

The time course of enantioselective hydrolysis of (*R,S*)-DMPM in different concentrations by employing PAE07 is shown in Fig. S4. The reaction was conducted under the following optimization: phosphate buffer (pH 8.0), temperature 40 °C, 10 mM PAE07 and 50–500 mM (*R,S*)-DMPM. When the substrate concentration was 50 mM, the yield of (*R*)-MAP-acid could reach 49.5% only after 70 min with *e.e.* value of 99.9%. Even when the concentration increased to 500 mM, the conversion could reach 49% after 10 h with $e.e._p$ value of 99.1%. The reaction times for conversion > 49% toward 100 mM, 250 mM and 350 mM (*R,S*)-DMPM were 120, 240, and 380 min, respectively, and the $e.e._p$ values were all more than 99%.

### 3.10. Homology modelling and docking study

To gain the molecular understanding of PAE07 of the excellent activity and selectivity of PAE07, a homology model of PAE07 was built based on the crystal structures of *N*-acyl homoserine lactonase from *Ochrobactrum* sp. T63 (PDB: 4G9E and 4G8D). The overall structure of the PAE07 model has a two-domain architecture that contained a core domain in the α/β-hydrolase fold and a cap domain (Fig. 4a). The core domain consisted of an eight-stranded β-sheet surrounded by seven α-helices and the cap domain was composed of five α-helices. The two domains were linked by loop 122–131 and loop 196–199. The classic catalytic triad Ser99/His249/Asp220 (Fig. 4b) of PAE07 was located at the interface between the core and cap domains. The whole active site is covered by the cap domain. The substrates of (*R*)-DMPM and (*S*)-DMPM were docked in the substrate bind area (8 Å surrounding the catalytic triad) using Autodock vina. The catalytic nucleophile residue Ser99 in the conserved motif GxSxG was nucleophilically attacked on the substrate ((*R*)-DMPM). Asp220 and His249 served as acidic and basic members of the catalytic triad, respectively. The distances from $-OCH_3$ to Ser99 and from $-OCH_3$ to His249 were 2.4 Å and 3.3 Å, respectively. The binding energy was −7.2 kcal/mol. The docking of (*S*)-DMPM into the substrate binding pocket was restricted due to the steric hindrance by the surrounding aromatic amino acids of Tyr159, Phe190, Phe137 and Phe222. Overall, the docking confirmation was in good agreement withthe detected strict *R*-selectivity of PAE07 toward (*R,S*)-DMPM.

In conclusion, a novel esterase (PAE07) gene was identified from the genomic DNA of *P. asaccharolyticum* WZZ003. The PAE07 enzyme exhibited high activity on C2 and C4 esters and excellent kinetic parameters toward *p*-NPA (the model substrate). The optimal temperature and pH of PAE07 were 40 °C and 8.0, respectively for the biotransformation on (*R,S*)-DMPM to (*R*)-MAP acid. Furthermore, PAE07 exhibited good thermostability. The enzyme activity remains > 60% after 2 h incubation at 60 °C. PAE07 demonstrated high catalytic efficiency and specific activity toward (*R,S*)-DMPM and high enantioselectivity ($e.e._p$ > 99%). Therefore, PAE07 is a competitive candidate for (*R*)-metalaxyl manufacturing.

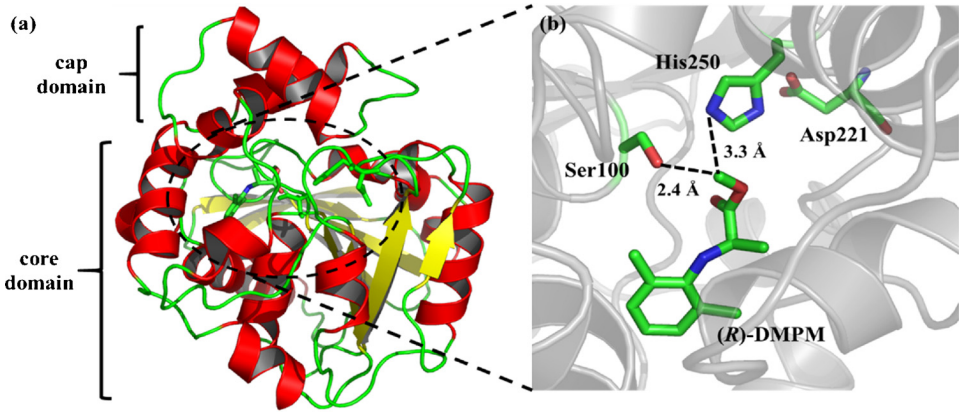


**Fig. 4.** Overall structure of modeled PAE07 (a) and the zoom view of its substrate binding site (b). The structure is shown in cartoon format and the key residues and (*R*)-DMPM are represented in stick format.

## Conflict of interest

The authors declare no financial or commercial conflict of interest.

## Acknowledgements

This study was funded by National Natural Science Foundation of China (31600639 and 31660247), Zhejiang Provincial Natural Science Foundation (LY18B020021), Zhejiang Provincial Qianjiang Talent project, and Zhejiang Provincial Xinmiao Talents Project (2017R403090).

## Appendix A. Supplementary data

Supplementary data associated with this article can be found, in the online version, at https://doi.org/10.1016/j.procbio.2018.03.011.

## References

[1] X.M. Wang, Y.J. Bai, Y.J. Cai, X.H. Zheng, Biochemical characteristics of three feruloyl esterases with a broad substrate spectrum from *Bacillus amyloliquefaciens* H47, Process Biochem. 53 (2016) 109–115.
[2] B.D. Ma, H.L. Yu, J. Pan, J.Y. Liu, X. Ju, J.H. Xu, A thermostable and organic-solvent tolerant esterase from *Pseudomonas putida* ECU1011: catalytic properties and performance in kinetic resolution of α-hydroxy acids, Bioresour. Technol. 133 (2013) 354–360.
[3] H. Dong, F. Secundo, C. Xue, X.Z. Mao, Whole-cell biocatalytic synthesis of cinnamyl acetate with a novel esterase from the DNA Library of *Acinetobacter hemolyticus*, J. Agric. Food Chem. 65 (2017) 2120–2128.
[4] L.D. Ye, H.N. Xu, H.W. Yu, Enhanced acylation activity of esterase BioH from *Escherichia coli* by directed evolution towards improved hydrolysis activity, Biochem. Eng. J. 79 (2013) 182–186.
[5] E. Topakas, C. Vafiadi, P. Christakopoulos, Microbial production, characterization and applications of feruloyl esterases, Process Biochem. 42 (2007) 497–509.
[6] M.C.A. Mukdsi, C. Haro, S.N. González, R.B. Medina, Functional goat milk cheese with feruloyl esterase activity, J. Funct. Foods 5 (2013) 801–809.
[7] L. Jiang, B. Wang, R.R. Li, S. Shen, H.W. Yu, L.D. Ye, Catalytic promiscuity of *Escherichia coli* BioH esterase: application in the synthesis of 3,4-dihydropyran derivatives, Process Biochem. 49 (2014) 1135–1138.
[8] B. Chankvetadze, Enantioseparation of chiral drugs and current status of electromigration techniques in this field, J. Sep. Sci. 24 (2015) 691–705.
[9] K. Yao, L. Zhu, Z.H. Duan, Z.Z. Chen, Y. Li, Z.S. Zhu, Comparison of R-metalaxyl and rac-metalaxyl in acute, chronic, and sublethal effect on aquatic organisms: *Daphnia magna*, *Scenedesmus quadricanda*, and *Danio rerio*, Environ. Toxicol. 24 (2009) 148–156.
[10] O.J. Park, S.H. Lee, T.Y. Park, S.W. Lee, K.H. Cho, Enzyme-catalyzed preparation of methyl(R)-N-(2,6-dimethylphenyl)alaninate: a key intermediate for (R)-metalaxyl, Tetrahedron. Asymmetry 16 (2005) 1221–1225.
[11] H.U. Blaser, C. Malan, B. Pugin, F. Spindler, H. Steiner, M. Studer, Selective hydrogenation for fine chemicals: recent trends and new developments, Adv. Synth. Catal. 345 (2003) 103–151.
[12] O.J. Park, S.H. Lee, Stereoselective lipases from *Burkholderia* sp. cloning and their application to preparation of methyl(R)-N-(2,6-dimethylphenyl)alaninate, a key intermediate for (R)-metalaxyl, J. Biotechnol. 120 (2005) 174–182.
[13] O.J. Park, S.H. Lee, T.Y. Park, W.G. Chung, S.W. Lee, Development of a scalable process for a key intermediate of (R)-metalaxyl by enzymatic kinetic resolution, Org. Process Res. Dev. 10 (2006) 588–591.
[14] J.H. Hung, Z. Weng, Sequence alignment and homology search with BLAST and ClustalW, Cold Spring Harb. Protoc. 11 (2016) pdb.prot093088.
[15] F. Cheng, L. Zhu, H. Lue, J. Bernhagen, U. Schwaneberg, Directed arginine deiminase evolution for efficient inhibition of arginine-auxotrophic melanomas, Appl. Microbiol. Biotechnol. 99 (2015) 1237–1247.
[16] Q.Q. Tian, P. Song, L. Jiang, S. Li, H. Huang, A novel cephalosporin deacetylating acetyl xylan esterase from *Bacillus subtilis* with high activity toward cephalosporin C and 7-aminocephalosporanic acid, Appl. Microbiol. Biotechnol. 98 (2014) 2081–2089.
[17] I. Navarro-González, S.F. Alvaro, G.C. Francisco, Overexpression purification, and biochemical characterization of the esterase Est0796 from *Lactobacillus plantarum* WCFS1, Mol. Biotechnol. 54 (2013) 651–660.
[18] T.C. Maester, M.R. Pereira, E.G. Machado Sierra, A. Balan, E.G. de Macedo Lemos, Characterization of EST3: a metagenome-derived esterase with suitable properties for biotechnological applications, Appl. Microbiol. Biotechnol. 100 (2016) 5815–5827.
[19] G. López, J. Chow, P. Bongen, B. Lauinger, J. Pietruszka, A novel thermoalkalostable esterase from *Acidicaldus* sp. strain USBA-GBX-499 with enantioselectivity isolated from an acidic hot springs of *Colombian Andes*, Appl. Microbiol. Biotechenol. 98 (2014) 8603–8616.
[20] K. Tamura, G. Stecher, D. Peterson, A. Filipski, S. Kumar, MEGA6: molecular evolutionary genetics analysis version 6.0, Mol. Biol. Evol. 30 (2013) 2725–2729.
[21] S. Kumar, G. Stecher, K. Tamura, MEGA7: molecular evolutionary genetics analysis version 7.0 for bigger datasets, Mol. Biol. Evol. 33 (2016) 1870–1874.
[22] M.A. Marti-Renom, A. Stuart, A. Fiser, R. Sánchez, F. Melo, A. Sali, Comparative protein structure modeling of genes and genomes, Annu. Rev. Biophys. Biomol. Struct. 29 (2000) 291–325.
[23] A. Gao, G.Y. Mei, S. Liu, P. Wang, Q. Tang, Y.P. Liu, H. Wen, X.M. An, L.Q. Zhang, X.X. Yan, D.C. Liang, High-resolution structures of AidH complexes provide insights into a novel catalytic mechanism for N-acyl homoserine lactonase, Acta Crystallogr. Sect. D 69 (2013) 82–91.
[24] R. Quiroga, M.A. Villarreal, A scoring function based on Autodock Vina improves scoring, docking, and virtual screening, PLoS One 11 (2016) e0155183.
[25] O. Trott, A.J. Olson, AutoDock Vina: improving the speed and accuracy of docking with a new scoring function, efficient optimization, and multithreading, J. Comput. Chem. 31 (2010) 455–461.
[26] C. Lee, J. Kim, S. Hong, B. Goo, S. Lee, S.H. Jang, Cloning, expression, and characterization of a recombinant esterase from cold-adapted *Pseudomonas mandelii*, Appl. Biochem. Biotechnol. 169 (2013) 29–40.
[27] A.J. Nicoll, R.K. Allemann, Nucleophilic and general acid catalysis at physiological pH by a designed miniature esterase, Org. Biomol. Chem. 2 (2004) 2175–2180.
[28] A. Çolak, D. Şişik, N. Saglam, S. Güner, S. Çanakçi, A.O. Beldzüz, Characterization of a thermoalkalophilic esterase from a novel thermophilic bacterium, *Anoxybacillusgonensis* G2, Bioresour. Technol. 96 (2005) 625–631.
[29] Y. Yang, J. Yang, B. Li, E. Wang, H. Yuan, An esterase from *Penicillium decumbens* P6 involved in lignite depolymerization, Fuel 15 (2018) 416–422.
[30] A. Kumar, V. Randhawa, V. Acharya, K. Singh, S. Kumar, Amino acids flanking the central core of Cu,Zn superoxide dismutase are important in retaining enzyme activity after autoclaving, J. Biomol. Struct. Dyn. 34 (2016) 475–485.
[31] J. Kim, S. Kim, S. Yoon, E. Hong, Y. Ryu, Improved enantioselectivity of thermostable esterase from *Archaeoglobus fulgidus* toward (*S*)-ketoprofen ethyl ester by directed evolution and characterization of mutant esterases, Appl. Microbiol. Biotechnol. 99 (2015) 6293–6301.
[32] C. Chen, Zhe Chi, G. Liu, H. Jiang, Z. Hu, Z. Chi, Production, purification, characterization and gene cloning of an esterase produced by *Aureobasidium melanogenum* HN6.2, Process Biochem. 53 (2017) 69–79.
[33] K. Rumbold, P. Biely, M. Mastihubová, M. Gudelj, G. Gübitz, K.H. Robra, B.A. Prior, Purification and properties of a feruloyl esterase involved in lignocellulose degradation by *Aureobasidium pullulans*, Appl. Environ. Microbiol. 69 (2003) 5622–5626.
[34] G. Degrassi, B.C. Okeke, C.V. Bruschi, V. Venturi, Purification and characterization of an acetyl xylan esterase from *Bacillus pumilus*, Appl. Environ. Microbiol. 64 (1998) 789–792.